Production of Oxygen Gas and Liquid Metal by Electrochemical Decomposition of Molten Iron Oxide

Dihua Wang,[a,b] Andrew J. Gmitter,[a,c,*] and Donald R. Sadoway[a,,z]**

[a]*Department of Materials Science and Engineering, Massachusetts Institute of Technology, Cambridge, Massachusetts 02139-4307, USA*
[b]*School of Resource and Environmental Sciences, Wuhan University, China*

Molten oxide electrolysis (MOE) is the electrolytic decomposition of a metal oxide, most preferably into liquid metal and oxygen gas. The successful deployment of MOE hinges upon the existence of an inert anode capable of sustained oxygen evolution. Herein we report the results of a program of materials design, selection, and testing of candidate anode materials and demonstrate the utility of iridium in this application. An electrolysis cell fitted with an iridium anode operating at 0.55 A cm^{-2} produced liquid metal and oxygen gas by the decomposition of iron oxide dissolved in a solvent electrolyte of molten MgO–CaO–SiO$_2$–Al$_2$O$_3$. The erosion rate of iridium was measured to be less than 8 mm y^{-1}. The stability of iridium is attributed to a mix of mechanisms including the electrochemical formation and simultaneous thermal decomposition of a surface film of iridium oxide.
© 2011 The Electrochemical Society.   [DOI: 10.1149/1.3560477] All rights reserved.

Modern metals extraction technologies face difficult environmental challenges. With worldwide steel production exceeding 1×10^9 tonnes annually,[1] the amount of byproduct carbon dioxide that accompanies steelmaking (>1.5 tonnes CO$_2$ per tonne of steel) is noteworthy on the scale of anthropogenic greenhouse gas (GHG) emissions.[2] The electrolytic production of aluminum also leads to generation of GHGs in the form of CO$_2$, CF$_4$, and C$_2$F$_6$ owing to the use of a consumable carbon anode (∼1.5 tonnes CO$_2$ per tonne of aluminum). In response, Sadoway has advocated molten oxide electrolysis (MOE) as a carbon-free alternative to existing metals extraction technology.[3] MOE is the electrolytic decomposition of a metal oxide, most preferably into liquid metal and oxygen gas. Early efforts to produce metal by oxide electrolysis go back more than 100 years,[4] but with few exceptions the process has not succeeded in moving beyond the confines of the laboratory.[5] More recently, variants of MOE have been studied with the intention of exploiting indigenous resources on the moon and on Mars for the generation of oxygen along with the production of structural metals such as iron and photovoltaic materials such as silicon.[6–13] At this point, the success of MOE hinges upon the existence of an inert anode capable of sustained oxygen evolution.

Previous work in this laboratory on inert anodes for aluminum-producing Hall–Héroult cells led to the enunciation of a set of selection criteria for the identification of materials for use as anodes in the fluoride-based electrolyte.[14] By analogy, in a molten oxide electrolyte an oxygen-evolving inert anode would desirably be composed of a material with the following attributes:

- physically stable (preferably solid) at service temperature.
- resistant to chemical attack by the molten oxide electrolyte.
- resistant to chemical attack by pure oxygen.
- electrochemically stable.
- electronically conductive.
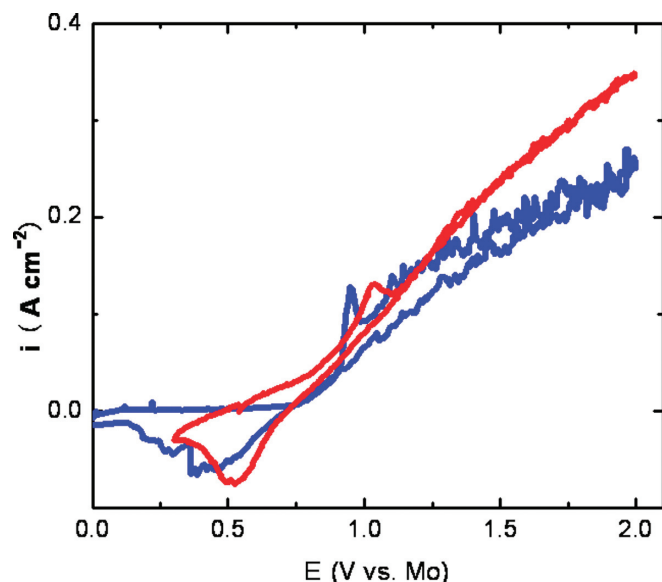- resistant to thermal shock.
- mechanically robust.

In addition, the material should be easy to deploy at industrial scale; for example, practicalities such as electrical connection to the bus, cell startup, response to loss of electrical power, etc., should be straightforward. Application of these selection criteria resulted in the choice of iridium. The performance of this material as an inert anode for MOE was assessed in the context of iron production by electrolysis of FeO dissolved in an alumino-silicate supporting electrolyte of composition MgO(16 wt %)–CaO(18 wt %)–Al$_2$O$_3$(20 wt %)–SiO$_2$ (46 wt %).

* Electrochemical Society Student Member.
** Electrochemical Society Active Member.
[c] Present address: Rutgers University, New Brunswick, NJ.
[z] E-mail: dsadoway@mit.edu

Experimental

Chemicals and equipment.—Powders of lime, magnesia, alumina, and silica (all from Alfa Aesar) were stored at 100°C with desiccant to prevent adsorption of water and agglomeration. 200 g batches were dry milled with no milling media in 500 mL Nalgene jars for roughly 24 h to thoroughly mix. The dry, mixed powders were poured into an alumina crucible (80 mm OD) or a molybdenum crucible (60 mm OD). The crucible was set into another alumina crucible and then placed into the bottom of a vertical closed-one-end alumina tube reactor (113 mm OD × 105 mm ID × 750 mm L, McDanel) in a vertical tube furnace heated by molybdenum disilicide elements (Mellen). The electrolyte was blanketed by flowing argon introduced via a mullite tube positioned in the hot zone of the furnace. The furnace was ramped at 85°C/h to 1575°C, and the contents were allowed to equilibrate for roughly one hour prior to electrochemical measurements.

Cyclic voltammetry.—The reference electrode was a 3.17 mm diameter Mo rod shrouded in a mullite tube. The counter electrode was identically prepared. Two kinds of working electrodes were used: (1) 0.5 mm diameter Ir wire connected to a 0.368 mm diameter Pt wire; (2) 3.17 mm diameter Mo rod. The exact electrode area exposed to the electrolyte was determined by a relation between current increment and electrode area increment (can be controlled from the top of the working electrode) at a specific electrode potential. Cyclic voltammetry with 70% *iR* compensation was used for all electrochemical measurements. Higher compensation values resulted in instability of the system.

Electrolysis and materials characterization.—Constant current electrolysis was conducted with an electrolyte of composition MgO (26 wt %)–CaO (25 wt %)–SiO$_2$ (49 wt %) (S1) or MgO (16 wt %)–CaO (18 wt %)–Al$_2$O$_3$ (20 wt %)–SiO$_2$ (46 wt %) (S1A) to which was added either 5 or 10 wt % FeO. A Mo rod (3.17 or 6.34 mm in diameter) was used as the cathode; an Ir plate (5 × 1 × 40 mm) or Ir wire (0.5 mm in diameter, 9.5 mm in length) served as the anode. The Ir plate was welded to a Mo rod which served as the current lead. The Ir wire anode was connected to a Pt wire, which served as the current lead. The Ir that served as the active anode was weighed before and after electrolysis. The entrained electrolyte on the anode was removed by immersing it in 47–51% HF aqueous solution. After electrolysis the Ir anode and the cathode metal product were examined by SEM and EDS (JEOL 5910).

Results

Figure 1 shows the results of cyclic voltammetry on an iridium wire, 0.5 mm diameter, at oxidizing potentials capable of generating oxygen gas. The blue trace represents data taken in the supporting

Figure 1. (Color online) CVs of an Ir wire (diameter 0.5 mm) working electrode in molten S1A [MgO(16 wt %)–CaO(18 wt %)–Al$_2$O$_3$(20 wt %)–SiO$_2$ (46 wt %)] without (blue line) and with 5 wt % FeO (red line) at 1575°C with a potential scan rate of 100 mV/s, reference electrode and counter electrode: Mo rods (3.17 mm in diameter).

Figure 2. (Color online) CVs of a Mo working electrode in molten S1 [SiO$_2$ (49 wt %)–CaO (25 wt %)–MgO (26 wt %)] with (red line) and without (green line) 5 wt % FeO 1575°C in a Mo crucible with a potential scan rate of 50 mV/s, reference electrode and counter electrode: Mo rods (3.17 mm in diameter).

electrolyte (S1A), while the red trace represents data taken in the same melt to which 5 wt % FeO has been added. At potentials less than 0.75 V (vs. MoO$_3$/Mo)[d], the blue trace shows near zero current indicating that iridium is electrochemically stable and that the electronic conductivity of the melt is negligible. At potentials exceeding 1.05 V the current grows measurably, and exhibits significant fluctuation on the order of 10 s of millivolts, which is consistent with gas evolution, i.e., formation, coalescence, and detachment of bubbles. In addition, there is a feature between 0.75 and 1.05 V, for which the peak current was found to be scan-rate dependent. This feature is assigned to the electrochemical formation of iridium oxide, which will be discussed below. Such putative behavior is similar to that observed during anodic oxidation of platinum in molten silicates as reported by Higgins[15,16] where he suggests the formation of an intermediate platinum oxide. The red trace in Fig. 1 shows that even upon addition of FeO to the alumino-silicate supporting electrolyte the electrical signatures of both oxygen evolution and putative iridium oxide formation are present. The positive slope in the current response at potentials lower than 0.75 V may be due to increasing electronic conductivity of the melt or oxidation of some Fe^{2+} which could result in polaron hopping between Fe^{2+} and Fe^{3+}. The higher oxygen evolution current is attributed to the greater concentration of free oxide ions in the FeO-bearing melt.

Figure 2 shows the results of a voltammetric study of iron deposition at 1575°C using a molybdenum rod working electrode. The green trace represents data taken in the supporting electrolyte (S1), while the red trace represents data taken in the same melt to which 5 wt % FeO has been added. The electrochemical window of the supporting electrolyte extends in the cathodic direction to –0.6 V at which potential the observed current is assigned to the electrodeposition of liquid silicon. Since, on thermodynamic grounds,[17] the onset of silicon deposition should occur at potentials roughly 0.3 V more cathodic than observed in Fig. 2, the data indicate underpotential deposition, which is not surprising given that silicon and molybdenum readily alloy at this temperature,[18] as do iron and molybdenum. In the anodic direction, an oxidation current is observed at potentials exceeding 0 V and is assigned to the oxidation of molybdenum itself.
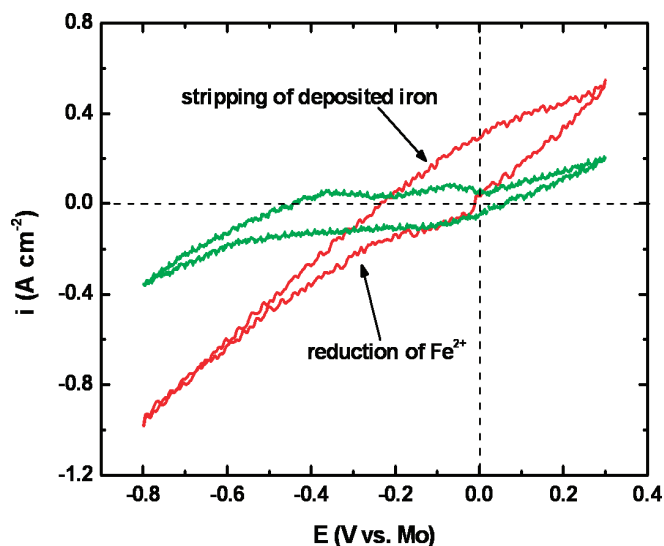
In contrast, the red trace representing the voltammogram of the electrolyte containing 5 wt % FeO shows a strong reduction current on the cathodic sweep at potentials as high as –0.05 V, in excellent agreement with the –0.08 V value from thermodynamic calculation, and in conformity with the electroreduction of Fe^{2+}.

Galvanostatic electrolysis was performed at a current density of 0.55 A cm^{-2} for a period of 6.35 h on a melt composed of the alumino-silicate supporting electrolyte containing 5 wt % FeO. An iridium wire, 0.5 mm diameter, 9.5 cm long, immersed 1.4 cm into the melt, served as the anode, while a molybdenum rod, 3.17 mm diameter, served as the cathode. The cell was also fitted with a reference electrode consisting of a molybdenum rod, 3.17 mm diameter. Temperature was set at 1575°C. The black trace of Fig. 3 shows that the potential on the anode as measured between it and the reference electrode remained nearly constant. The condition of the iridium
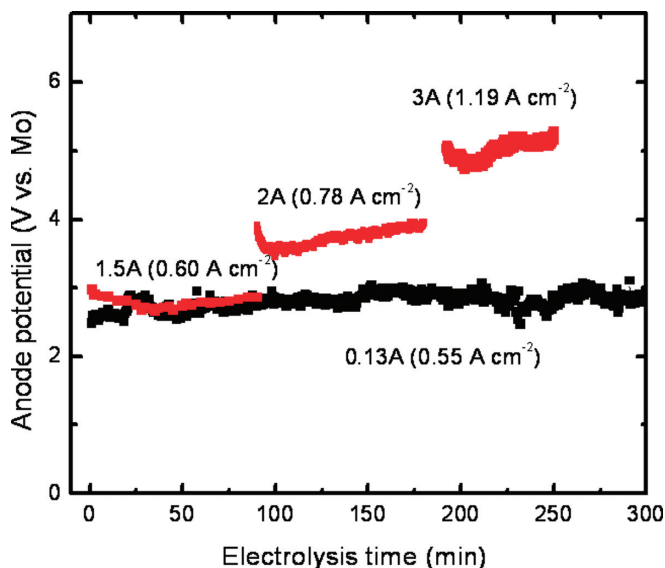
Figure 3. (Color online) Variation of potential with time of an Ir wire anode (black line, 0.5 mm diameter, 1.4 cm in melt) in S1A with 5 wt % FeO at 1575°C and of an Ir plate anode (red line, area: 2.52 cm^2) in S1A with 10 wt % FeO at 1575°C during constant current electrolysis.

[d] All potentials are reported against a MoO$_3$/Mo pseudo-reference electrode.

(a)   (b)
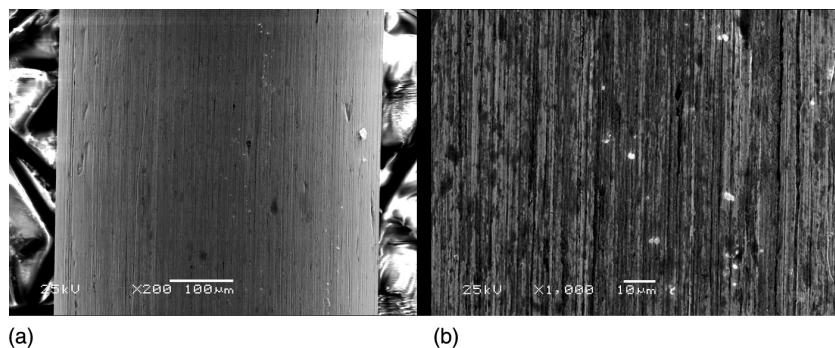
Figure 4. SEM image of original Ir wire anode (0.5 mm in diameter) before (a) and after (b) electrolysis for 6.35 h in S1A + 5 wt % FeO at 1575°C with an anodic polarization current density of 0.55 A cm^{-2}.

anode is depicted before and after electrolysis (the entrained electrolyte was removed by immersing the iridium wire in 47–51% HF aqueous solution for 45 min) in Figs. 4a and 4b, respectively, showing a change in surface finish but no perceptible change in diameter. The mass of the iridium wire was 440.13 and 437.12 mg before and after electrolysis, respectively. The 3.01 mg weight loss of the entire iridium wire is equivalent to a consumption rate of ∼7.7 mm/year when ascribed only to the section of wire immersed in the electrolyte. According to the standards set forth by the aluminum industry (less than 10 mm/year, the only industrial specification available[19]) such a wear rate qualifies for the designation of inert anode. However, if one accounts for anode consumption above the melt line by thermochemical oxidation of iridium and sublimation of the iridium oxide so formed,[20] the 7.7 mm/year figure can be viewed as an upper bound, i.e., the erosion rate of the anode immersed in the melt is less than this value. Subsequent testing of an anode made of iridium plate, 40 × 5 × 1 mm, confirmed the initial findings. In this second experiment the electrolyte contained 10 wt % FeO dissolved in the alumino-silicate supporting electrolyte. Cell voltage was seen to be stable even as current density was varied from 0.60 to 1.19 A cm^{-2} as seen in the red traces of Fig. 3. After electrolysis the plate thickness was visibly unchanged, and no iridium was detected by EDS and XPS in the cathode product or in the electrolyte frozen on anode. The bulk electrolyte far from the anode was not searched for evidence of elemental iridium. The metal on the cathode was determined by EDS to be an alloy of iron and molybdenum. Electrochemical generation of oxygen was confirmed by chemical analysis of gas evolving on the anode (Model O2 Oxygen Analyzer, Oxigraf, Inc., Mountain View, CA) and swept away in an argon flow. By the same method no oxygen was detected when no current passed through the cell.
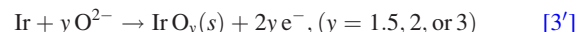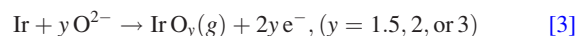
Discussion

On the basis of these experimental data we put forth the following scheme to explain the performance of iridium as an oxygen-evolving inert anode in iron-bearing alumino-silcate melts. The overall half-cell reactions during the electrolysis of FeO are
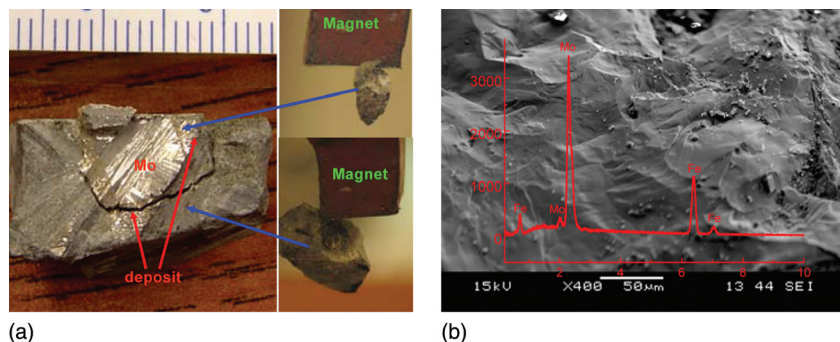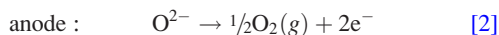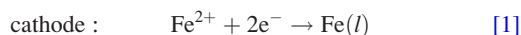
$$\text{cathode}: \quad Fe^{2+} + 2e^- \rightarrow Fe(l) \qquad [1]$$

$$\text{anode}: \quad O^{2-} \rightarrow \tfrac{1}{2}O_2(g) + 2e^- \qquad [2]$$

At the anode, we speculate that the mechanisms at work include the following, where the term, melt, refers to the molten oxide electrolyte

- electrochemical oxidation of iridium to form iridium oxide (iridia), which is a gas at this temperature

$$Ir + y\,O^{2-} \rightarrow Ir\,O_y(g) + 2y\,e^-, (y = 1.5, 2, \text{ or } 3) \qquad [3]$$

$$Ir + y\,O^{2-} \rightarrow Ir\,O_y(s) + 2y\,e^-, (y = 1.5, 2, \text{ or } 3) \qquad [3']$$

- dissolution of iridia in the molten oxide electrolyte

$$IrO_y(g) + MO_z(melt) \rightarrow MIrO_{y+z}(melt) \qquad [4]$$

$$IrO_y(g) \rightarrow IrO_y(melt) \qquad [4']$$

- decomposition of iridia into its constituent elements

$$IrO_y(g) \rightarrow Ir(electrode) + 0.5y\,O_2(g) \qquad [5]$$

$$IrO_y(g) \rightarrow Ir\ (dispersed\ in\ the\ melt) + 0.5yO_2(g) \qquad [5']$$

- electrochemical dissolution of iridium, i.e., electrostripping

$$Ir \rightarrow Ir^{4+}(melt) + 4e^- \qquad [6]$$
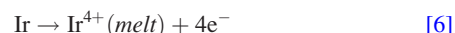
In Fig. 1, we see in the feature between 0.75 and 1.05 V possible evidence for Reaction 3 or Reaction 6. If Reaction 3 is operative then the fate of such electrochemically generated iridia on the anode surface determines the utility of the anode. Any of the following reactions would consume iridia and thereby deplete the anode of material: dissolution (Reactions 4 and 4′), decomposition (Reaction 5′), or fugitive emission (Reaction 3). The exception is Reaction 5 which does not result in the removal of iridium from the anode. In fact, if the rate of thermal decomposition of iridia according to Reaction 5 occurs at a rate that exceeds the rate of iridia generation by Reaction 3, this will result in the continuous release of oxygen gas which bubbles away and the continuous release of iridium metal which remains on the anode. Evidence for the latter can be seen in Fig. 4b which reveals surface reconstruction of the iridium without loss of material. Such an iridium electrode would be termed an iridia-mediated inert anode (IMIA), or more generally an oxide-mediated inert anode (OMIA). Alternatively, if $k_2 \gg k_i$, where $i = 3$–6, we should expect the same outcome.

(a)   (b)
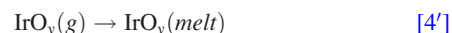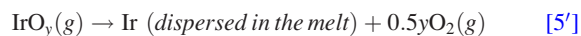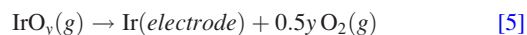
Figure 5. (Color online) (a) Photo image showing deposit on a hanging Mo cathode (6.3 mm in diameter) after electrolysis of S1A melt containing FeO and (b) SEM image of deposit and EDS analysis (superimposed in red) of same.

The concept of an oxide-mediated inert anode should not be limited to iridium metal and molten oxide melts; in principle, the anodic behavior of other noble metals including Pt, Rh, Au, and Ag may be explained to the extent that they form an intermediate compound by chemical combination with a constituent of the electrolyte in conformity with the set of reactions set forth above. Thus, one might possibly be able to obtain an inert anode by adjusting relative rates of Reactions 3–6 through control of temperature, electrolyte composition, and metal alloy composition. Given that in halide melts oxygen evolution occurs at less extreme potentials than does halogen evolution, we speculate on the potential utility of an oxide-mediated inert anode for other metallurgical processes of interest.

In summary, by presenting results for electrochemical decomposition of FeO dissolved in an alumino-silicate melt to produce oxygen gas and liquid metal at 1575°C we have demonstrated that iridium can serve as an oxygen-evolving anode in an oxide melt at extremely high temperature. Several mechanisms have been put forth to explain the performance of iridium and to provide guidance to future efforts at inert anode development in other electrolytic systems. While iridium is far too costly and its natural abundance in the earth's crust is far too low to meet the needs of the world steel industry, iridium has an important role to play in laboratory-scale studies of electrolytic cells evolving oxygen and in specialized settings such as in situ generation of oxygen in extraterrestrial venues.

Acknowledgments

References

1. *World Steel in Figures*, World Steel Association, Brussels (2010).
2. E. Worrell, L. Price, and N. Martin, *Energy (Oxford, U. K.)*, **26**, 513 (2001).
3. D. R. Sadoway, *J. Mater. Res.*, **10**, 487 (1995).
4. R. H. Aiken, U.S. Pat. 816142 (1906).
5. R. Winand, A. Fontana, L. Segers, P. Hannaert, and J. Lacave, in *Molten Salt Electrolysis Metal Production International Symposium*, The Institution of Mining and Metallurgy, London, pp. 42–50, (1977).
6. R. O. Colson and L. A. Haskin, in Resources of Near-Earth Space, J. S. Lewis, M. S. Matthews and M. L. Guerrieri, Editors, pp. 109–27, University of Arizona Press, Tucson (1993).
7. D. G. Kesterke and S. P. Nasa, NASA Spec. Publ. (NASA SP-229), pp. 139–44 (1970).
8. D. G. Kesterke, U.S. Bur. Mines, Rep. Invest. (RI 7587), p. 12 (1971).
9. D. Khetpal, A. C. Ducret, and D. R. Sadoway, *NASA Conf. Publ.*, **2003–212339**, 548 (2003).
10. D. J. Lindstrom and L. A. Haskin, *Lunar Planet. Sci.*, **10**, 733 (1979).
11. M. J. Oppenheim and H. Tabor, *Adv. Space Sci. Technol.*, **11**, 233 (1972).
12. A. H. C. Sirk, D. R. Sadoway, and L. Sibille, *ECS Trans.*, **28**(6), 367 (2010).
13. A. T. Vai, J. A. Yurko, D. H. Wang, and D. R. Sadoway, in *Jim Evans Honorary Symposium*, B. Q. Li, B. G. Thomas, L. Zhang, F. M. Doyle, and A. P. Campbell, Editors, pp. 301–308, TMS, Warrendale, PA (2010).
14. D. R. Sadoway, Light Metals 1990: Advances in Aluminum Production, C. A. Bickert, Editor, pp. 403-07, TMS, Warrendale, PA (1990).
15. J. K. Higgins, *Glass Technol.*, **21**, 145 (1980).
16. J. K. Higgins, *Glass Technol.*, **23**, 90 (1982).
17. A. Roine, *HSC Chemistry 6.0*, Outokumpu Technology, Pori, Finland (2006).
18. A. B. Gokhale and G. J. Abbaschian, *J. Phase Equilib.*, **12**, 493 (1991).
19. *Inert Anode Roadmap*, U.S. Department of Energy, Washington, DC (1998).
20. H. Jehn, R. Voelker, and M. I. Ismail, *Platinum Met. Rev.*, **22**, 92 (1978).